Velocity correlations in a one-dimensional lattice gas: Theory and simulations

T. Naitoh* and M. H. Ernst
Institute of Theoretical Physics, University of Utrecht, P.O. Box 80006, 3508 TA Utrecht, The Netherlands

M. A. van der Hoef and D. Frenkel
FOM–Institute for Atomic and Molecular Physics, Kruislaan 407, 1098 SJ Amsterdam, The Netherlands
(Received 29 December 1992)

In a one-dimensional fluid the macroscopic Navier-Stokes equations are no longer valid because of long-time tails and diverging transport coefficients. By performing computer simulations on a one-dimensional cellular automaton fluid we have investigated the ranges of times and densities where the intermediate- and long-time behavior of the velocity correlation function is correctly described by mode-coupling theory. The agreement is in general surprisingly good.

PACS number(s): 05.20.Dd, 02.70.−c, 05.40.+j, 05.60.+w

I. INTRODUCTION

Is a one-dimensional fluid too pathological to be described in terms of hydrodynamic concepts? The answer is a conditional no, as we shall show in this paper. In the context of lattice-gas cellular automata (LGCA's), there exist several models [1], whose dynamics conserve total momentum, thus ensuring that the average flow velocity $u(r,t)$ is a slow hydrodynamic variable.

In such a fluid, the only possible slow modes are the two sound modes. However, one expects that the "transport coefficients" describing the damping of the sound waves, $\nu\nabla^2 u$, are more strongly divergent than in two-dimensional fluids [2]. Consequently even the form of the dissipative terms in the fluid-dynamic equations is unknown.

For the one-dimensional model, to be considered in this paper, there is evidence from theory and computer simulations for the existence of these divergences, either obtained by measuring the attenuation of long-wavelength sound [1] or by directly simulating the stress-stress correlation function [2,3]. In the former case it was found that the damping constant $\nu(k)\sim k^{-\alpha}$ diverges with $\alpha\simeq 0.3$–0.5 [1–3] in the long-wavelength limit instead of approaching a finite transport coefficient ν_0. In the latter case, direct simulations of the stress-stress correlation function have shown that its time integral $\nu(t)\sim t^{\beta}$ diverges as $t\to\infty$, except for the half-filled lattice. A self-consistent mode-coupling calculation suggests that $\beta=\frac{1}{3}$, but the existing one-dimensional simulations are too noisy to make any quantitative comparison [3]. Recently, Naitoh and Ernst [4] have considerably improved the statistics by taking on the order of 10^6 runs per density point. Their results give strong indications that a tail with an exponent $\beta=\frac{1}{3}$, as compared to $\beta=\frac{1}{2}$, gives a better fit to the simulation data, but their results are not yet conclusive. Here however, the extremely high accuracy of the moment-propagation method [5–8] enables us to study the velocity autocorrelation function (VACF) of a tagged particle in this fluid, but not the stress-stress correlation function.

Obviously, the VACF should approach zero for long times, possibly through power-law decay. However, when performing computer simulations on our one-dimensional cellular-automaton (CA) fluid, the VACF of a tagged particle appeared to approach to *a negative constant,* as illustrated in Fig. 1 for a system of 500 lattice sites on a line. It was this remarkable observation, suggesting the existence of some type of conserved quantity, that motivated the present research.

Our objective is not only to give a quantitative explanation of this constant anticorrelation in one-dimensional systems, but also to investigate the full time dependence of the VACF from kinetic relaxation to the long-time tail regime, using mode-coupling theory. This theory assumes that the long-time relaxation can be described through the decay of products of hydrodynamic modes [9,10]. In particular, the combination of a shear mode and a self-diffusion mode leads to the asymptotic long-time tail $t^{-d/2}$ of the VACF [2,6] for $d\geq 2$.

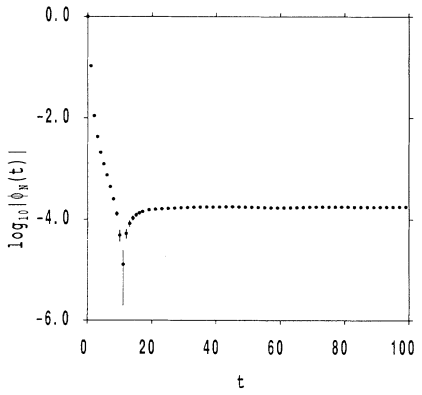

FIG. 1. The simulated VACF in the one-dimensional self-dual five-bits model at $f=0.7$ and $L=500$. The logarithm of $|\phi_N(t)|$ is shown vs time t. Note that the $\phi_N(t)$ is *negative* for $t\geq 12$.

 ©1993 The American Physical Society

However, there are no shear modes in one-dimensional systems. Therefore mode-coupling theory will be formulated (i) to include the sound modes, which yields subleading asymptotic tails in higher-dimensional systems; and (ii) to account for finite-size effects by restricting the allowed wave numbers to the discrete set, determined by the periodic boundary conditions.

In a previous publication, this extended mode-coupling theory for finite systems has been compared in great detail with computer simulations on LGCA's in two and three dimensions [11], and even in four dimensions [12]. In the present paper, this mode-coupling theory will be compared with computer simulations on the so called five-bits model, a LGCA defined on a line, where particles can have five different velocities.

II. MODE-COUPLING THEORY

Mode-coupling studies on the long-time behavior of the VACF $\langle \mathbf{v}(t)\cdot\mathbf{v}(0)\rangle$ in LGCA's have been considered in Refs. [1–8]. The current of a tagged particle is interpreted as $\sum_{\mathbf{r}} u_x(\mathbf{r},t)P(\mathbf{r},t)$, with $u_x(\mathbf{r},t)$ the local fluid velocity and $P(\mathbf{r},t)$ the concentration of tagged particles. The time dependence of these slowly varying fields is calculated from the diffusion equation and the hydrodynamic equations, where the flow field is decomposed into shear modes and sound modes. In the present case, we also take the sound modes into account. By a minor extension of the methods of Refs. [2,5] one obtains for the normalized VACF $\psi_N(t)=\langle \mathbf{v}(t)\cdot\mathbf{v}\rangle/\langle v^2\rangle$ the following mode-coupling result:

$$\psi_N(t)=\frac{(1-f)}{dN}\left\{(d-1)\sum_{\mathbf{q}}\exp[-(D+\nu)q^2t]+\sum_{\mathbf{q}}\cos(c_0qt)\exp[-(D+\tfrac{1}{2}\Gamma)q^2t]\right\}, \tag{2.1}$$

where $N=\rho V$ is the number of fluid particles in a LGCA defined on a regular space lattice with V sites and b possible velocities per site. The reduced density is defined as $f=\rho/b$, with $0<f<1$. The sound velocity c_0 in a b-bits athermal LGCA is given by $dbc_0^2=\sum_c c^2$, and D, ν, and Γ denote respectively the self-diffusion coefficient, the kinematic viscosity, and the sound-damping constant. For classical fluids one finds Eq. (2.1), with $(1-f)$ replaced by unity [13]. This factor is a consequence of the Fermi exclusion rule in lattice gases. The first term, containing the contributions from the shear modes, is absent in one dimension. For $d=1$ and 2, the transport coefficients are replaced by bare transport coefficients D_0, ν_0, Γ_0, given by the short-time or Boltzmann approximation [9,10]. For superlong-time tails, Eq. (2.1) leads to inconsistencies [10,14].

In the thermodynamic limit ($V\to\infty$) all $O(N^{-1})$ terms disappear and the $\mathbf{q}$ sum in Eq. (2.1) is replaced by an integral over all $\mathbf{q}$ space,

$$\phi(t)=\frac{(1-f)v_0}{bfd(4\pi t)^{d/2}}\left\{(d-1)\left[\frac{1}{D+\nu}\right]^{d/2}+\left[\frac{1}{(D+\frac{1}{2}\Gamma}\right]^{d/2}{}_1F_1\left[\frac{d}{2},\frac{1}{2},-\frac{t}{t_h}\right]\right\}, \tag{2.2}$$

where $t_h=4(D+\frac{1}{2}\Gamma)/c_0^2$ is the hydrodynamic relaxation time, v_0 is the volume of the unit cell, and ${}_1F_1$ is the confluent hypergeometric function. The first term of Eq. (2.2) is the leading long-time tail obtained in [5] (absent in the case of $d=1$), and the second one represents the subleading contributions involving the sound modes. For dimensionality $d=1$, the confluent hypergeometric function reduces to ${}_1F_1(\frac{1}{2},\frac{1}{2}-z)=e^{-z}$ and therefore the sound-mode contributions are exponentially damped.

However, to discuss the finite-size effects in Eq. (2.1), it is instructive to transform the reciprocal-lattice sum in Eq. (2.1) back to a sum over the direct lattice using the formula

$$\sum_{\mathbf{q}}\exp[-i\mathbf{q}\cdot\mathbf{r}]\exp[-q^2/4\rho^2]=\frac{v_0(\rho L)^d}{\pi^{d/2}}\sum_{\mathbf{l}}\exp[-|\mathbf{l}L-\mathbf{r}|^2\rho^2]\ . \tag{2.3}$$

Equation (2.3) represents a periodic function of $\mathbf{r}$ with a period L in d-space directions. It is a d-dimensional generalization of a well-known formula in the theory of lattice vibrations [15]. The left-hand sum extends over all lattice points $\mathbf{l}$ of an infinite regular space lattice, and the right-hand sum runs over all lattice points $\mathbf{n}$ of the corresponding infinite reciprocal lattice with $\mathbf{q}=2\pi\mathbf{n}/L$.

For a one-dimensional system, formula (2.3) allows us to transform (2.1) into an equivalent representation,

$$\psi_N(t)=\left[\frac{1-f}{bf}\right]\left\{\frac{1}{\sqrt{4\pi(D+\frac{1}{2}\Gamma)t}}\sum_{n=-\infty}^{n=\infty}\exp\left[-\frac{L^2}{4(D+\frac{1}{2}\Gamma)t}\left[\frac{c_0t}{L}-n\right]^2\right]\right\}. \tag{2.4}$$

It is a superposition of Gaussian wave packets, initially excited in each replica of the system and propagating with the speed of sound.

In computer simulations on LGCA's, one uses an equilibrium molecular-dynamics (MD) ensemble with a fixed number of particles N, one of which is tagged, and a fixed total momentum $\mathbf{P}=\mathbf{0}$. The VACF obtained in this ensemble will be denoted by

$$\phi_N(t)=\langle \mathbf{v}(t)\cdot\mathbf{v}(0)\rangle_{\mathrm{MD}}/\langle v^2\rangle_{\mathrm{MD}}\ . \tag{2.5}$$

In the canonical ensemble used to derive Eq. (2.1), one has $\langle \mathbf{P}\rangle=\mathbf{0}$, but the ensemble contains systems with

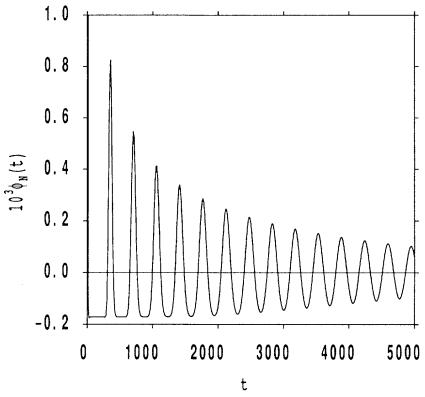

FIG. 2. The finite-hydrodynamics prediction for the VACF at $f=0.7$ and $L=500$ for t on the order of 14 acoustic traversal times.

P≠0. Both correlation functions ψ_N and ϕ_N can be related by identifying ϕ_N with the VACF in the center-of-mass frame, i.e.,

$$\langle v^2\rangle\phi_N(t)=\langle \mathbf{v}'(t)\cdot\mathbf{v}'\rangle=\langle \mathbf{v}(t)\cdot\mathbf{v}\rangle-\langle P^2\rangle/N^2 , \tag{2.6}$$

where $\mathbf{v}'=\mathbf{v}-\mathbf{P}/N$. The momentum fluctuation is given by $\langle P^2\rangle=N(1-f)\langle v^2\rangle$, where the factor $(1-f)$ follows from the Fermi exclusion rule. The two VACF's are therefore related by

$$\phi_N(t)=\psi_N(t)-(1-f)/N . \tag{2.7}$$

In the thermodynamic limit, both functions approach the infinite-system result (2.2). However, their long-time behavior at finite N is quite different. Inspection of (2.1) shows that all terms decay exponentially except for the term ($\mathbf{q}=\mathbf{0}$), that yields $(1-f)/N$. So $\psi_N(\infty)=(1-f)/N$ and $\phi_N(\infty)=0$. The function $\phi_N(t)$ in mode-coupling approximation is therefore given by Eq. (2.1), with the term ($\mathbf{q}=0$) excluded from the summations. As an illustration of the theoretical results, we have calculated the lattice sum (2.1) numerically for our one-dimensional model (to be described in the next section), with a speed of sound $c_0=\sqrt{2}$ contained in a volume of $V=L=500$ lattice sites with periodic boundary conditions, and we have plotted in Fig. 2 the function $\phi_N(t)$, corresponding to the simulation data, over a time period of about 14 acoustic traversal times. The acoustic traversal time here is $t_a=L/c_0\simeq 354$. A discussion of this remarkable behavior and a comparison with simulation results is the subject of the next section.

III. CA FLUID ON A LINE

We consider the self-dual five-bits model introduced by d'Humières, Lallemand, and Qian [1], which is an athermal CA fluid in one dimension. Shear modes are absent and only sound modes contribute to Eq. (2.1). Finite-size effects are expected to be more significant than in higher-dimensional models. The system in this model consists of $V=L$ lattice points on a line. At each lattice point there are five velocity channels ($c=0,\ \pm1,\ \pm2$; $b=5$), each of which can be occupied by at most one particle. The collision rules for these particles are self-dual (particle-hole symmetry),

$$\begin{aligned}
&(-1)+(+1)+(0)^\dagger \Longleftrightarrow (-2)+(+2)+(0)^\dagger ,\\
&(0)+(-1)+(+2)^\dagger \Longleftrightarrow (+1)+(-2)+(+2)^\dagger ,\\
&(0)+(+1)+(-2)^\dagger \Longleftrightarrow (-1)+(+2)+(-2)^\dagger ,
\end{aligned} \tag{3.1}$$

where $(i)^\dagger$ represents collisions taking place irrespective of the presence of a "spectator" particle with velocity i at the same lattice point. The collision rules for a tagged particle are only different from those of fluid particles in the sense that the outgoing tagged particle is scattered with equal probability into any allowed outgoing velocity channel [6]. Consequently, in the limit of a completely filled lattice ($f=1$), the tagged particle performs a random walk with equal probabilities for each of five displacements, $\Delta=0,\ \pm1,\ \pm2$. Hence the diffusion coefficient is $D=\frac{1}{2}[\frac{2}{5}\times1+\frac{2}{5}\times4]=1$, and the VACF vanishes for all $t\geq1$. For general densities, no exact results for the transport coefficients are known.

To compare our simulation results for this model, we need the speed of sound $c_0=\sqrt{2}$, as follows from $bdc_0^2=\sum_c c^2$ for athermal LGCA's, and the transport coefficients. In the Boltzmann approximation, the sound-damping constant Γ_0 [1] and self-diffusion coefficient D_0 [2,16] are given by

$$\begin{aligned}
&\Gamma_0=\nu_0=\frac{3}{10f(1-f)}-\frac{7}{10} ,\\
&D_0=c_0^2\left[\frac{1}{\lambda}-\frac{1}{2}\right] ,\\
&\lambda=1-[(1-b)f]^{-1}(1-f)[1-(1-f)^{b-1}] ,
\end{aligned} \tag{3.2}$$

with $b=5$. The VACF in the Boltzmann approximation is given [16] by the exponential function, $\phi_B(t)=(1-\lambda)^t\equiv\exp(-t/t_0)$ which defines the mean free time t_0.

We first return to Fig. 1 and consider the simulation data for $\phi_N(t)$, obtained for a system of $L=500$ sites at reduced density $f=0.7$. The data show three different types of behavior in the time interval considered: an exponential decay for $t\leq2$ which is well described by the Boltzmann approximation $\phi_B(t)$; another exponential decay for $3<t<15$ which is expected to be explained by the sound-mode contributions, and a *negative plateau* for $t>20$, which clearly shows the finite-size effects. The initial exponential decay is not very well visible in Fig. 1. The two distinct exponential regimes are more clearly exhibited in Fig. 3, where $\log_{10}[\psi_N(t)]=\log_{10}[\phi_N(t)+(1-f)/N]$ is plotted versus t for a rather large system of $L=2000$ sites at reduced density $f=0.7$. In Fig. 3, the simulation data are also compared with the mode-coupling prediction (2.2) for the infinite one-dimensional system (solid line in Fig. 3), i.e.,

$$\phi(t)\simeq\frac{(1-f)}{5c_0f\sqrt{\pi t_h t}}\exp(-t/t_h) . \tag{3.3}$$

Here the hydrodynamic relaxation time $t_h\simeq3.1$ indicates

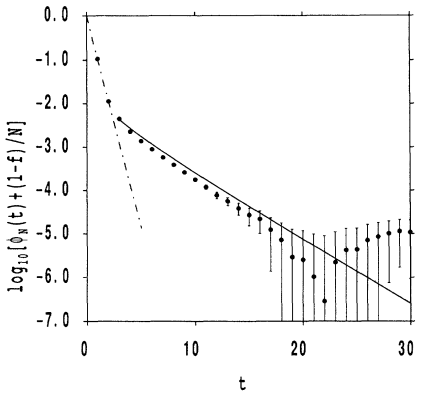

FIG. 3. The logarithm of $\psi_N(t)=\phi_N(t)+(1-f)/N$ vs time in a one-dimensional model for system size $L=2000$ at density $f=0.7$. The symbols ●'s represent the results of computer simulations. The solid and dotted curves denote results obtained, respectively, from (extended-) infinite-mode-coupling theory in Eq. (2.2) and the finite hydrodynamics in Eq. (2.1).

the crossover from kinetic relaxation, $\phi_B(t)=\exp(-t/t_0)$, with $t_0=0.45$, to hydrodynamic relaxation.

Next we interpret the theoretical result of Fig. 2, which contain only sound-mode contributions. It is instructive to consider the finite hydrodynamics result $\phi_N(t)$ transformed back to real space, as given by Eq. (2.4). This formula is very well suited to discuss the behavior of $\phi_N(t)=\psi_N(t)-(1-f)/N$ in the time interval $2<t<t_a$, where $t_a=L/c_0$ is the acoustic traversal time. The right-hand side of Eq. (2.4) is a superposition of an infinite number of Gaussian wave packets, traveling with the speed of sound, initially excited in each replica and produced by the periodic boundary conditions. The time difference between the adjacent peaks is given by the acoustic traversal time t_a. The width of these peaks is increasing as $\sqrt{4(D+\frac{1}{2}\Gamma)t}$ due to the diffusion of the tagged particle and the damping of sound modes. The relative magnitude of the peak separation and peak width determines whether the negative plateau or the damped oscillations can be observed in a specific time region. In particular, in the time interval satisfying the inequalities

$$\sqrt{4(D+\tfrac{1}{2}\Gamma)t} \ll c_0 t \ll L \quad \text{or} \quad t_h < t < t_a \ , \tag{3.4}$$

$\psi_N(t)$ vanishes and $\phi_N(t)$ shows very markedly a *negative plateau,* given by the opposite of the $q=0$ term, i.e., $\phi_{\text{plat}}=-(1-f)/N$. Here the spreading $\sqrt{4(D_0+\frac{1}{2}\Gamma_0)t}$ of the wave packets is small compared to the propagation distance $c_0 t$ and simultaneously $t<t_a$. For times t much larger than the acoustic traversal time, $\phi_N(t)$ again approaches zero.

To verify the predictions, we carried out a simulation up to much longer times, and obtained the results shown in Figs. 4(a)–4(c). There is excellent agreement between simulations and theory. In the data of Fig. 4(a) for the $L=500$ system (triangles), there is a negative plateau for $25<t<275$, and another one for $t\geq 430$. They are separated by a sharp peak, occurring at the acoustic traversal time $t_a=L/c_0=354$. This constant anticorrela-

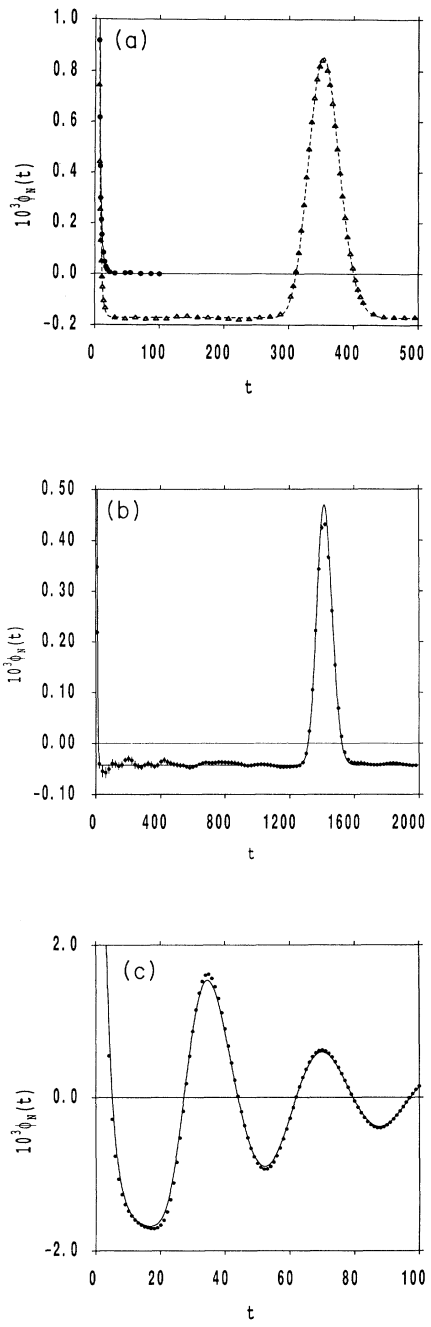

FIG. 4. (a) The simulated values of the VACF in the one-dimensional model for $L=500$(▲) and $L=10^5$ (●) at $f=0.7$. The dotted curve shows the finite hydrodynamics prediction for $L=500$. The solid curve represents the extended mode-coupling prediction (2.2) for an infinite system. The simulation data and finite hydrodynamics results clearly exhibit the *negative plateau.* (b) The VACF in the one-dimensional model at $f=0.7$ and $L=2000$. The solid curve represents the finite hydrodynamics prediction and the dots represent computer simulations. Both results show much wider negative plateaus than those in (a). (c) The VACF in the one-dimensional model at $f=0.7$, and $L=50$. The solid curve represents the finite hydrodynamics prediction and the black dots represent computer simulations. Both results show damped oscillations.

tion can be understood as follows. Since the tagged particle is given an initial velocity of c, and the ensemble is prepared in such a way that the total momentum vanishes, each fluid particle has on the average a velocity $-c/N$, yielding the anticorrelation $\phi_{\text{plat}}=-(1-f)c_0^2/N$, where the factor $(1-f)$ comes from the Fermi exclusion. In the time interval satisfying Eq. (3.4), the fluid momentum (without the tagged particle) is essentially a constant of motion. Figure 4(a) also shows the simulation data for a system of $V=L=10^5$ lattice sites (black circles) at the same density. Here finite-size effects are completely negligible and the simulations coincide with the theoretical result Eq. (2.2) for the infinite system (solid line). Again, there is excellent agreement between simulations and the extended mode-coupling theory. Similar results, shown in Fig. 4(b), are obtained for the larger system of $L=2000$ sites at $f=0.7$, with an acoustic traversal time $t_a=1414$.

To confirm the damped oscillations in Fig. 2, we performed a simulation for much longer times on a much smaller system of $L=50$, with $t_a=35.4$, in which the VACF is expected to give damped oscillations at much earlier times than in the $L=500$ system. The mode-coupling results, shown in Fig. 4(c), are again in excellent agreement with the computer simulations. The oscillations are due to interference effects of the tails of the diffusive sound-wave packets, which have already arrived in the reference region from its neighboring replicas.

The negative plateau value $\phi_{\text{plat}}=(1-f)/N$ may also be viewed as an effective finite-size correction, applied to the simulation data, i.e., the "corrected data" are $\psi_N(t)=\phi_N(t)+\phi_{\text{plat}}$. The reason is that ψ_N and ϕ_N are given by the unconstrained and constrained $\mathbf{q}$ sum in Eq. (2.2), respectively, including and excluding the term $(\mathbf{q}=\mathbf{0})$. The unconstrained sum gradually approaches to the $\mathbf{q}$ integral of the infinite system, given by (2.2) or (3.3). Therefore, in Fig. 5 we show the same data as in Figs. 4(a) and 4(c) in a logarithmic plot, which gives a blowup of 100 times the VACF values in Fig. 4 in the range of t values of 20–30 time steps. This illustrates the extent to which the data for different system sizes can be collapsed with the result for the thermodynamic limit. Collapse is obviously restricted to time intervals $t<\frac{1}{2}t_a$, guaranteeing the absence of all interference effects of sound waves with their periodic images. For system sizes $L=50$ and 500, these times are approximately 18 and 177.

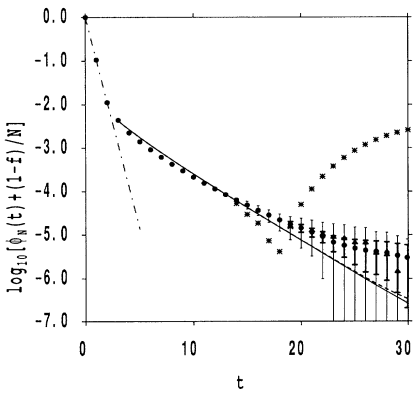

FIG. 5. The corrected data for finite hydrodynamics and MD data at different system sizes, $\psi_N(t)=\phi_N(t)+(1-f)/N$ at $f=0.7$ ($*$ for $L=50$, $\triangle$ for $L=500$, and $\bullet$ for $V=10^5$), are collapsed with the infinite system result $\phi(t)$ [solid line, Eq. (2.2)]. The finite hydrodynamic prediction (2.1) are shown as dashed lines. The standard deviations are denoted by thin vertical lines ($L=500$) and thick ones ($L=10^5$).

Indeed, Fig. 5 shows the collapse of the corrected MD data for different system sizes with the infinite system result (2.2) in the appropriate time interval $t\leq 17$. For the smallest system ($L=50$), the MD data (denoted by an asterisk and shown without error bars) and the finite hydrodynamics results should deviate from the infinite system curve for $t\geq\frac{1}{2}t_a$, as explained in Fig. 4, but they remain in agreement with the mode-coupling theory at finite N [see Fig. 4(c)]. In the remaining data, the error bars increase strongly for $t>17$ because theory predicts that $\phi_N(t)$ becomes *negative* for $t\geq 12$ (MD 11), 15 (MD 14), and 26 (MD 84) for the system sizes $L=500$, 2000, and 10^5, respectively. The numbers (MD x) denote the observed zero crossings in the MD simulations. The quantity $\phi_{\text{corr}}=\phi_N+(1-f)/N$ vanishes exponentially fast and becomes small compared to the absolute errors, which are of order 10^{-6} for all system sizes.

Finally, in Fig. 5 we note that the very large system data ($L=10^5$) start to decay more slowly than described by the mode-coupling theory with bare transport coefficients after about 20 time steps. This might be an indication of divergent transport coefficients, as discussed in the Introduction. The self-diffusion coefficient in a one-dimensional fluid does not seem to diverge, because the time integral over the VACF (3.3) is expected to converge as long as the longitudinal viscosity $\nu(t)\sim t^{\beta}$ is growing more slowly than linearly ($\beta<1$). Of course one should realize that we have reached the limits of our statistical accuracy when the correlation function has decayed to about one 10^{-5} of its initial value. For $t>20$, the relative error in the uncorrected data $\phi_N(t)$ rapidly increases from 25% ($t=22$), to 70% ($t=25$) and to 130% ($t=30$).

To substantiate the expected relation between the above deviations and the divergence of one-dimensional transport coefficients, a short discussion of the stress-stress correlation function is required. The long-time behavior of the one-dimensional stress-stress correlation function (whose time sum determines the longitudinal viscosity or sound damping) behaves very differently from the one-dimensional VACF, according both to the simulations and to mode-coupling theory [2,3]. For the VACF, the contributions of the diffusion and sound modes lead in one dimension to the exponentially decaying result (3.3).

In the stress-stress correlation function $\phi_\nu(t)$, two opposite sound modes combine to produce an algebraic long-time tail, $d_0 t^{-\alpha}$, with an exponent α. The theoretical prediction from bare mode-coupling theory (supposedly applicable on some intermediate time scale) is $\alpha=\frac{1}{2}$. The asymptotic self-consistent mode-coupling theory predicts $\alpha=\frac{2}{3}$ [2]. Measurements of sound-wave damping in computer simulations seem to suggest $\alpha\simeq 0.5$. [1]. Direct simulation of the stress-stress corre-

lation function of sufficient statistical accuracy are not yet available.

The longitudinal viscosity itself, $\nu(t)=\sum_{\tau=0}^{t}\varphi_\nu(t)$, diverges as $d_0 t^{1-\alpha}/(1-\alpha)$. However, the amplitude d_o of the tail is proportional to some power of $|1-2f|$, which therefore *vanishes* for the half-filled lattice, because the amplitude of the tail is vanishing. Consequently, the longitudinal viscosity is not expected to diverge for the half-filled lattice. If the deviations of the MD data from mode-coupling theory for $t>18$ in the large system ($L=10^5$ in Fig. 5) are indeed related to the divergence of the viscosity, then simulations of the same statistical accuracy for the half-filled lattice should not show such deviations. This is indeed the case, as illustrated in Fig. 6 for density $f=\frac{1}{2}$ and system size $L=10^5$.

We also remark that there exist some unexplained small, but systematic deviations in the overall numerical factor between the long-time behavior of the MD data and the mode-coupling prediction (3.3). This occurs in the time interval ($3<t<18$ in Fig. 5 and $t>4$ in Fig. 6) where mode-coupling theory with bare transport coefficients is supposed to be valid.

In *summary,* we conclude that the simulated values of the VACF are well described by the mode-coupling theory with *bare* transport coefficients, including the finite-size effects and the interference effects from periodic boundaries. The bare mode-coupling theory breaks down after a crossover time t_c, where the divergence of the longitudinal viscosity seems to control the long-time behavior of the VACF. At the reduced density $f=0.7$, the crossover occurs after $t_c\simeq 20$ time steps, or approximately 45 mean free times.

The crossover argument is consistent with the simulation data for the half-filled lattice, where the longitudinal viscosity does not diverge, according to bare mode-coupling theory. Consequently the simulation data and the bare mode-coupling results should be and are indeed in agreement over the total time interval over which simulations could be carried out.

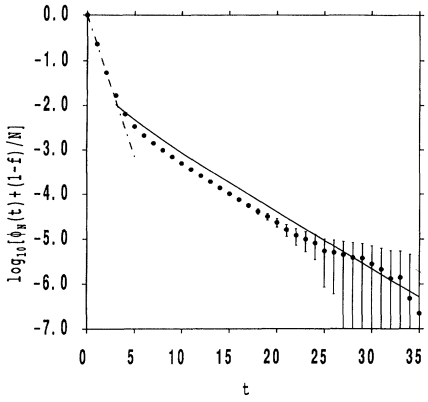

FIG. 6. The simulated VACF at density $f=\frac{1}{2}$ and system size $L=10^5$ compared with mode-coupling theory. The large time deviations between theory and simulations, seen in Fig. 5, are absent in the half-filled lattice, where algebraic tails are absent.

Recently (see [14]) evidence has been given that self-consistent mode-coupling theory is able to describe the superlong-time regime ($t>t_c$) in two-dimensional lattice gases. There are strong indications of the validity of self-consistent mode-coupling theory in one dimension, but a definite answer can only be given when more accurate simulations of the stress-stress correlation function become available.

ACKNOWLEDGMENTS

T.N. thanks the Institute for Theoretical Physics of the University of Utrecht for its kind hospitality during his stay. The work of the FOM Institute is part of the scientific program of FOM and is supported by the "Nederlandse Organisatie voor Wetenschappelijk Onderzoek" (NWO). Computer time on the NEC-SX2 at NLR was made available through a grant by NFS (National Fonds Supercomputers).

*On leave from Senshu University, Higashi-mita, Tama-Ku, Kawasaki 214, Japan.

[1] D. d'Humières, P. Lallemand, and Y. H. Qian, C. R. Acad. Sci. Paris II **308**, 585 (1988); Y. H. Qian, Ph.D. thesis, Université Pierre et Marie Curie, 1990.

[2] M. H. Ernst, Physica D **47**, 198 (1991).

[3] J. de Smet, M. H. Ernst, and D. Frenkel, Master's thesis, University of Utrecht, 1990.

[4] T. Naitoh and M. H. Ernst, in *Proceedings of the Sixth Conference on Molecular Physics, Kanazawa, Japan, 1992,* edited by K. Nakanishi and N. Quirke, Molecular Simulation (Gordon and Breach, New York, in press).

[5] D. Frenkel and M. H. Ernst, Phys. Rev. Lett. **63**, 2165 (1989).

[6] M. A. van der Hoef and D. Frenkel, Phys. Rev. A **41**, 4277 (1990); Physica D **47**, 191 (1991).

[7] M. A. van der Hoef, Simulation Study of Diffusion in Lattice-Gas Fluids and Colloids, Ph.D. dissertation, University of Utrecht, 1992.

[8] T. Naitoh, M. H. Ernst, M. A. van der Hoef, and D. Frenkel, in *Numerical Methods for Simulation of Multiple-Phase and Complex Flow,* edited by T. M. M. Verheggen, Springer Lecture Notes in Physics Vol. 398 (Springer-Verlag, Berlin, 1992), p. 29; T. Naitoh and M. H. Ernst, in *Discrete Models of Fluid Dynamics,* edited by A. S. Alves, Series on Advances in Mathematics for Applied Sciences (World Scientific, Singapore, 1991), p. 166.

[9] M. H. Ernst and J. W. Dufty, J. Stat. Phys. **58**, 57 (1990).

[10] T. Naitoh, M. H. Ernst, and J. W. Dufty, Phys. Rev. A **42**, 7187 (1990).

[11] T. Naitoh, M. H. Ernst, M. A. van der Hoef, and D. Frenkel, Phys. Rev. A **44**, 2484 (1991).

[12] M. A. Van der Hoef, M. Dijkstra, and D. Frenkel, Europhys. Lett. **17**, 39 (1992).

[13] J. J. Erpenbeck and W. W. Wood, Phys. Rev. A **26**, 1648 (1982).

[14] M. A. van der Hoef and D. Frenkel, Phys. Rev. Lett. **66**, 1591 (1991); J. A. Leegwater and G. Szamel, *ibid.* **67**, 408 (1991).

[15] J. M. Ziman, in *Principles of the Theory of Solids* (Cambridge University Press, Cambridge, England, 1972).

[16] M. H. Ernst and T. Naitoh, J. Phys. A **24**, 2555 (1991).